# Journal of Materials Chemistry C



PAPER

View Article Online

View Journal | View Issue



Cite this: *J. Mater. Chem. C*, 2023, **11**, 15657

# Anti-bonding mediated record low and comparable-to-air lattice thermal conductivity of two metallic crystals†

Zhonghua Yang, (1) ‡<sup>a</sup> Wenbo Ning, ‡<sup>a</sup> Alejandro Rodriguez, b Lihua Lu, a Junxiang Wang, a Yagang Yao, d Kunpeng Yuan (1) \* b Alejandro Rodriguez, b Lihua Lu, a Junxiang Wang, a Yagang Yao, d Kunpeng Yuan (1) \* b Alejandro Rodriguez, b Lihua Lu, a Junxiang Wang, a Junxiang Wa

In most pure metals and metallic systems, although the electronic thermal conductivity is believed to dominate thermal transport, the magnitude of lattice (phononic) thermal conductivity (LTC) is usually not negligibly low. We report two exceptional metallic materials, namely cubic half-Heusler-type PbAuGa and CsKNa, by solving the phonon Boltzmann transport equation (BTE) based on first-principles calculations. The two crystals possess record low LTCs of 0.064 W  $mK^{-1}$  and 0.031 W  $mK^{-1}$  at room temperature, respectively, among all pure metals and metallic systems we have known so far. Such LTCs, which are even comparable to that of air (about 0.025 W mK<sup>-1</sup> under ambient conditions), only contribute 0.37% and 0.29% to the overall thermal transport. By quantitatively characterizing both phonon-phonon and phonon-electron interactions, it is demonstrated that the anomalously low LTC stems from low group velocity and strong anharmonicity which can be traced back to anti-bonding nature at the electronic level. The acoustic modes of PbAuGa and CsKNa originating from Au and Cs respectively dominate the thermal transport. By examining the mean square displacement, potential energy well, and crystal orbital Hamiltonian population, we find that the magnitude of movement of loosely bonded Au and Cs atoms in PbAuGa and CsKNa respectively is appreciable, and the Au and Cs atoms act as intrinsic rattlers and thus induce strong phonon anharmonicity and ultrashort lifetime reaching the loffe-Regel limit. This study deepens our understanding of heat conduction in metals and metallic systems and provides a route for searching for novel materials with nearly zero lattice thermal conductivity for future emerging applications.

Received 26th August 2023, Accepted 12th October 2023

DOI: 10.1039/d3tc03064d

rsc.li/materials-c

#### 1. Introduction

The ability to predict and design thermal transport in bulk crystalline materials is of fundamental importance for a wide range of energy applications. In areas such as the development of thermal barrier coatings and thermoelectric devices, engineering materials with extremely low lattice (phononic) thermal conductivity ( $\kappa_1$ ) are vital. Thermal energy in crystal lattices can be carried through different vibrational modes, the so-called

quasi-particles (phonons), thus it is necessary to get an insight into the governing factors or intrinsic material features that limit the thermal transport, such as phonon harmonicity and anharmonicity. The modes of lattice vibration supported by harmonic crystals are noninteracting and propagate without decay. However, different modes of vibration interact with each other and propagate with decay in anharmonic crystals,2 and this process leads to a finite lifetime.<sup>3-5</sup> Rattling atoms are a well-known concept proposed for achieving intrinsically low  $\kappa_1$ , 6,7 where rattlers refer to specific atoms or atom clusters with large amplitude vibrations.8 In the materials with rattling atoms, the large space and weak bonding make the rattling atoms (guests) vibrate with larger displacement and different frequencies compared with atoms in the host framework. This kind of vibration yields additional scattering of phonons and reduces the thermal conductivity significantly. For example, ultralow κ<sub>1</sub> values of AgIn<sub>5</sub>S<sub>8</sub>, CuIn<sub>5</sub>S<sub>8</sub>, Rb<sub>2</sub>SnBr<sub>6</sub>, and CuP<sub>2</sub> are in the range of 0.1 W mK<sup>-1</sup>-0.74 W mK<sup>-1</sup> at room temperature and are induced by the rattling effect. 9-11

Recently, researchers did a lot of work to enhance the thermal conductivity of low-conductivity materials. Compounds with

<sup>&</sup>lt;sup>a</sup> College of Architecture and Civil Engineering, Shenyang University of Technology, Shenyang, 110870, China

<sup>&</sup>lt;sup>b</sup> Department of Mechanical Engineering, University of South Carolina, Columbia, 29201, USA. E-mail: hu@sc.edu

<sup>&</sup>lt;sup>c</sup> College of New Energy, China University of Petroleum (East China), Qingdao 266580, China. E-mail: yuankunpengupc@163.com

<sup>&</sup>lt;sup>d</sup> National Laboratory of Solid State Microstructures, College of Engineering and Applied Sciences, Jiangsu Key Laboratory of Artificial Functional Materials, and Collaborative Innovation Center of Advanced Microstructures, Nanjing University, Nanjing 210093, China

<sup>‡</sup> These authors contributed equally to this work.

structural disorder (e.g.,  $\kappa_1$  of SiGe alloys: 1 W mK<sup>-1</sup>-2 W mK<sup>-1</sup>12,13), soft bonds (e.g.,  $\kappa_1$  of GaP: 1.52 W mK<sup>-114</sup>), and complex atomic structures (e.g.,  $\kappa_1$  of Yb<sub>14</sub>MnSb<sub>11</sub>: 0.6 W mK<sup>-1 15</sup>) are thus favored since these features lead to low phonon velocities and strong phonon anharmonicity. 16 Despite of a large number of studies achieving lattice thermal conductivity of semiconductors and insulators at an extremely low level research on ultralow thermal conductivity of metals and metallic materials has received less attention. It is known that both phonons and electrons contribute to heat conduction in pure metals and metallic systems.<sup>17</sup> For most such materials, the electronic thermal conductivity ( $\kappa_e$ ) is believed to be much higher than the phononic thermal conductivity ( $\kappa_p$ ). At room temperature, the phononic thermal conductivity of typical pure metals and metallic structures ranges from 2 to 18 W mK<sup>-1</sup> which accounts for 1% to 40% of the total thermal conductivity. 18 This implies that, in most pure metals and metallic systems, although the electronic thermal conductivity is believed to dominate thermal transport, the magnitude of phononic thermal conductivity is usually not negligibly low. This motivates us to investigate the possibility of extremely low thermal conductivity of metals and metallic materials, e.g., on the level of less than  $0.1 \text{ W mK}^{-1}$ .

Recent advances in artificial intelligence (AI) techniques have significantly accelerated the discovery of materials with optimal properties for various applications, including superconductivity, catalysis, and thermoelectricity. 19-22 In our recent high-throughput prediction of the phonon transport properties of large-scale inorganic crystals based on deep learning, 22,23 after thoroughly screening 80 000 cubic crystals from the Open Quantum Materials Database (OQMD), 24,25 two metallic compounds, namely PbAuGa and CsKNa, are identified with anomalously low phononic thermal conductivity, having the lowest phononic thermal conductivity among all crystalline materials we have known so far. Obviously, the phononic thermal conductivity of metallic PbAuGa and CsKNa is well below the reasonable range. Therefore, a comprehensive analysis of the phononic and electronic thermal conductivity of PbAuGa and CsKNa is highly desirable. In this work, using first-principles calculations, in order to analyze and account for the anomalously low thermal conductivity of PbAuGa and CsKNa, two other common metallic materials Pd and Ag are also studied for comparison. The effect of both phononphonon (p-p) scattering and phonon-electron (p-e) scattering on phononic thermal conductivity is carefully quantified. Our study provides deep insight into the anomalously low thermal conductivity of PbAuGa and CsKNa and helps us to obtain a more general conclusion on heat conduction in metals, which is expected to have a broad impact on practical applications involving low lattice thermal conductivity materials.

### 2. Computational methods

Combining the Boltzmann transport equation (BTE) and Fourier's law, the phononic thermal conductivity can be calculated as:

$$\kappa_{\alpha} = \sum_{\lambda} c_{\text{ph},\lambda} \nu_{\alpha,\lambda}^{2} \tau_{\lambda} \tag{1}$$

where  $\kappa_{\alpha}$  denotes the lattice thermal conductivity in the  $\alpha$ th direction,  $\lambda$  represents a specific phonon mode with wave vector **q** and phonon branch **s**,  $\nu_{\alpha,\lambda}$  is the phonon group velocity of the mode  $\lambda$  along the  $\alpha$ th direction,  $\tau_{\lambda}$  is the phonon lifetime of the mode  $\lambda$ ,  $C_{ph,\lambda}$  refers to the phonon volumetric specific heat of the mode  $\lambda$  and is calculated as:

$$c_{\text{ph},\lambda} = \frac{k_{\text{B}}}{NV} \frac{\left(\hbar\omega_{\lambda}/k_{\text{B}}T^{2}\right) e^{\hbar\omega_{\lambda}/k_{\text{B}}T}}{\left(e^{\hbar\omega_{\lambda}/k_{\text{B}}T} - 1\right)^{2}} \tag{2}$$

where  $k_{\rm B}$  is the Boltzmann constant, N is the q-points number in the first Brillouin zone, V is the unit cell volume,  $\hbar$  is the reduced Planck constant, T is the absolute temperature, and  $\omega$  is the phonon angular frequency of the mode  $\lambda$ . The group velocity of the phonon mode  $\lambda$  is the gradient of frequency with respect to wave vector:

$$\nu_{\lambda} = \nabla_{\lambda} \omega_{\lambda} \tag{3}$$

The phonon lifetime is one of the key parameters determining the phononic thermal conductivity which can be obtained using Matthiessen's rule as:

$$\frac{1}{\tau_{\lambda}^{p}} = \frac{1}{\tau_{\lambda}^{pp}} + \frac{1}{\tau_{\lambda}^{pe}} \tag{4}$$

where  $\frac{1}{\tau^{pp}_{\cdot}}$  denotes the phonon–phonon (p–p) scattering rate

which is related to the three-phonon scattering matrix and  $\frac{1}{\tau^{pe}}$ denotes the phonon-electron (p-e) scattering rate which is related to the p-e scattering matrix.

First-principles calculations including density functional theory (DFT) and density functional perturbation theory (DFPT) are carried out using the Quantum Espresso (QE) package<sup>26</sup> to predict the phononic and electronic thermal transport in these metals by considering both p-p and p-e scatterings. The atomic structure is fully optimized to ensure the stability of the lattice structure. The Ultra Soft Pseudo Potential (USPP) is adopted and a 70 Ry planewave energy cutoff is used to expand the electronic wave functions. Both lattice constants and atomic coordinates are fully relaxed, and K-points of 21  $\times$  21  $\times$  21 and 13  $\times$  13  $\times$  13 gamma grids are set for pure metals (Pd, Ag) and metallic compounds (PbAuGa, CsKNa), respectively. The convergence criterion for energy and atomic force is set as  $1 \times 10^{-8}$  Ry and  $1 \times 10^{-7}$  Ry Bohr<sup>-1</sup>, respectively. In order to solve the problem of expensive computation for solids with large and complex unit cells, the approach named compressive sensing lattice dynamics (CSLD)<sup>27</sup> is used to obtain the 2nd and 3rd interatomic force constants (IFCs) for the phononic thermal conductivity calculation. We calculated the normalized trace of IFC tensors<sup>28</sup> which is used to describe the strength of interatomic iterations quantity [see Fig. S1 in the ESI†]. According to this parameter, one can directly determine how large the cutoff radius should be to evaluate the anharmonic IFCs by effectively including the possibly strong interaction strength as revealed by the large trace value. To this end, the cutoff radius has been set as 6.527 Å, 6.897 Å, 5.1516 Å, and 7.673 Å for Pd, Ag, PbAuGa and CsKNa, respectively, in this calculation. To get converged results with affordable computational cost, a 3  $\times$  3  $\times$  3

supercell with 2  $\times$  2  $\times$  2 K-points is used to obtain the IFCs of PbAuGa and CsKNa. More detailed computational parameters can be found in Table S1 in the ESI.†

In the p-e scattering rate calculations, the phonon perturbation is first calculated using DFPT as implemented in QE and then the p-e scattering matrix is calculated using the Electron-Phonon Wannier (EPW) package.29 The initial and final K-points and Q-grids are tested carefully to achieve convergence for electrical conductivity and thermal conductivity [see Table S2, ESI†]. To ensure the accuracy of the EPW package, the interpolated band structures obtained from EPW and ph.x modules in QE are compared in Fig. S2 (ESI†). The results indicate the reliability of the calculation. For lattice thermal conductivity calculations, the ShengBTE package<sup>30</sup> was modified to incorporate the p-e scattering and p-p scattering. The thermal conductivity convergence of PbAuGa and CsKNa with respect to the Q-grids is fully examined as shown in Fig. S3 (ESI†). It is shown in Fig. S3 (ESI†) that the thermal conductivity of PbAuGa converges when the Q-grids are greater than 15 imes 15 imes 15, and for CsKNa, the thermal conductivity does not change considerably over the different Q-grids tested and thus the Q-grid is set as  $20 \times 20 \times 20$  for this material.

#### 3. Results and discussion

The optimized structures of PbAuGa and CsKNa are illustrated in Fig. S4 (ESI†) which shows a typical cubic structure. Both materials have the same symmetry of  $F\overline{4}3m$  (space group number 216). The fully optimized lattice constants of the primitive cell and the angle between two lattice vectors are 4.747 Å and 60° for PbAuGa, and 7.063 Å and  $60^{\circ}$  for CsKNa, and the corresponding lattice constants of the conventional cell are a = b = c = 6.713 Å for PbAuGa and 9.989 Å for CsKNa. The primitive cell of PbAGa crystallizes in a rhombohedral lattice with Pb, Ga, and Ga atoms sitting along the diagonal direction, which is the same as CsKNa.

#### (1) Phononic thermal conductivity by only considering p-p scattering

To analyze and account for the heat transfer mechanism of PbAuGa and CsKNa, pure metals Pd and Ag which also have a cubic structure are added for comparison. By examining the nature of bonding and lattice vibrations, the phonon dispersion of Pd, Ag, PbAuGa, and CsKNa is plotted in Fig. 1. There are no imaginary frequencies in the phonon dispersion of both compounds PbAuGa and CsKNa, as shown in Fig. 1(c) and (d), respectively, implying their dynamical stability. Furthermore, our computed elastic constants and cohesive energy of materials are listed in Tables S3 and S4 (ESI†). From the tables, it is clear that the elastic constants and cohesive energy of both PbAuGa and CsKNa satisfy the mechanical and energetic stability criteria. Therefore, compounds PbAuGa and CsKNa are dynamically, mechanically, and energetically stable. In the PbAuGa system, the acoustic modes are dominated by the relatively heavier elements Pb and Au, and the phonon density

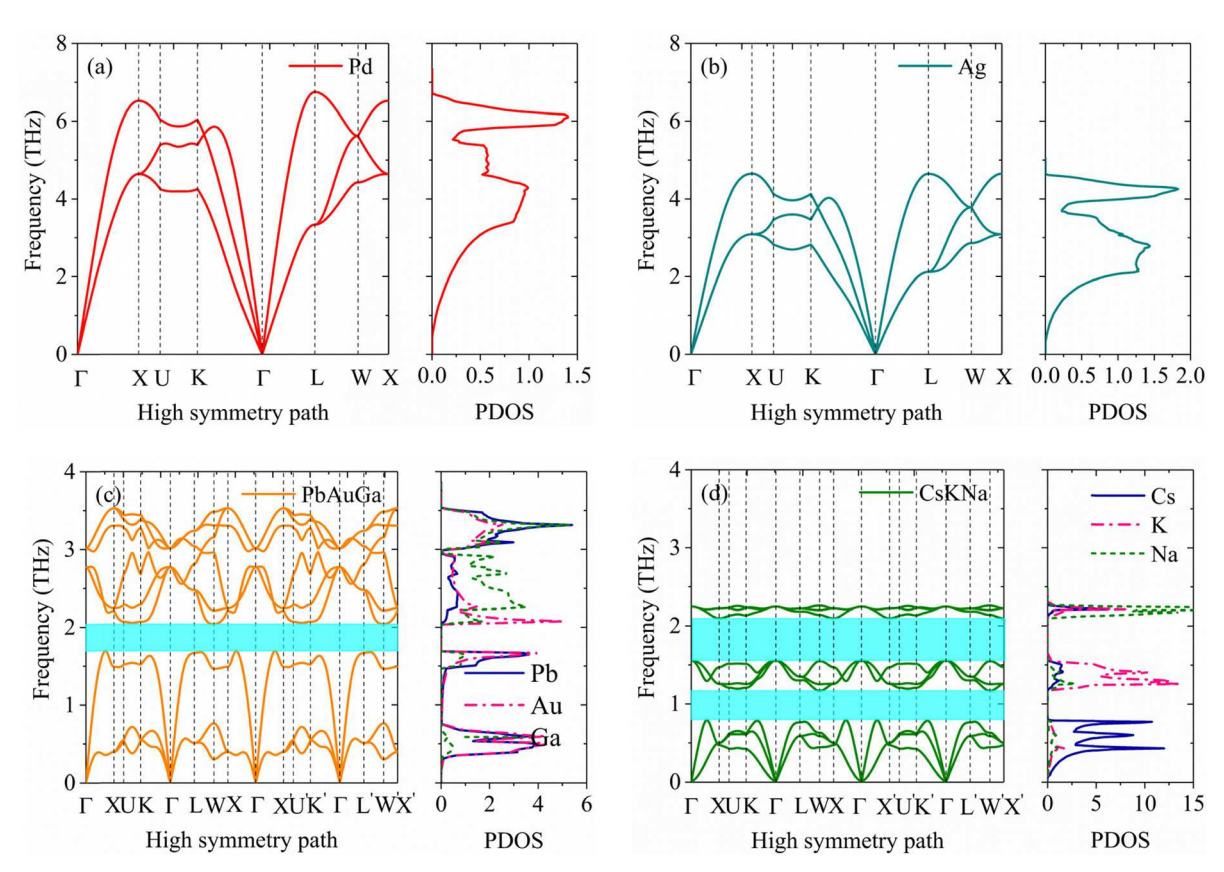


Fig. 1 Phonon dispersions (left panels) and partial phonon density of states (right panels) of (a) Pd, (b) Ag, (c) PbAuGa, and (d) CsKNa.

of states (PDOS) of Ga is concentrated in low-lying optical (LLO) modes and high-lying optical (HLO) modes. In CsKNa, the acoustic modes, LLO modes, and HLO modes are dominated by Cs, K, and Na, respectively, which is well expected considering their atomic mass decreases from high to low. Compared to the phonon dispersions of pure metal Pd and Ag, there exists a phonon frequency gap with a similar width between acoustic modes and low-lying optical modes naturally in PbAuGa and CsKNa (the shaded cyan area in Fig. 1), owing to their significant atom mass differences. CsKNa, in particular, exhibits very interesting features in its phonon dispersion as a second and broader phonon frequency gap is observed between the LLO modes and HLO modes.

The temperature-dependent  $\kappa_p^{p-p}$  of PbAuGa and CsKNa is illustrated in Fig. 2(a). The  $\kappa_p^{p-p}$  of Ag in the literature<sup>18</sup> is presented as a star as a reference, which agrees very well with our calculation. The  $\kappa_p^{p-p}$  decreases with the increase in temperature, which is the same behavior as most semiconductors and insulators. Strikingly, the  $\kappa_{\rm p}^{\rm p-p}$  of PbAuGa and CsKNa is extraordinarily low (0.064 W  $\mbox{mK}^{-1}$  and 0.031 W  $\mbox{mK}^{-1}$  at room temperature, respectively), which is about 2 orders of magnitude lower than that of pure metal Pd and Ag. Although many 3D (bulk) crystalline materials with ultralow lattice thermal conductivity (below 1 W mK<sup>-1</sup>) were reported in previous studies,  $^{31-34}$  the  $\kappa_{\rm p}^{\rm p-p}$  of PbAuGa and CsKNa is even several times lower than the previously reported lower bound, which is the most interesting part of this work. Specifically, the CsKNa crystal possesses a record low  $\kappa_{\rm p}^{\rm p-p}$  of 0.031 W mK<sup>-1</sup> at room temperature, the lowest among all pure metals and metallic systems and even semiconductors and insulators we have known so far. This low lattice thermal conductivity is even comparable to that of air (about 0.025 W mK<sup>-1</sup> under ambient conditions).

Based on eqn (1) and (2), the phonon volumetric specific heats of four systems are calculated for the sake of comparison. At room temperature (300 K), the phonon volumetric specific heats are as follows: Pd:  $0.26 \times 10^7$  J (m<sup>-3</sup> K<sup>-1</sup>), Ag:  $0.23 \times$  $10^7 \text{ J (m}^{-3} \text{ K}^{-1})$ , PbAuGa:  $0.16 \times 10^7 \text{ J (m}^{-3} \text{ K}^{-1})$ , and CsKNa:  $0.50 \times 10^6 \,\mathrm{J}\,(\mathrm{m}^{-3}\,\mathrm{K}^{-1})$ , respectively. Comparably speaking, the phonon volumetric specific heat of CsKNa is about 19% of Pd, which is much less than their difference in  $\kappa_p^{p-p}$ . Therefore, the volumetric specific heat should not be the governing factor for the lower lattice thermal conductivity of PbAuGa and CsKNa.

It is generally believed that electrons make a dominant contribution to the thermal transport of metals, while phonons contribute less. We comprehensively discuss phononic and electronic contributions to thermal transport in PbAuGa and CsKNa. Based on eqn (4), the phononic thermal conductivity in metals is influenced by both p-p and p-e scattering. To gain deeper insight into phononic thermal conductivity, we first investigate the phononic thermal conductivity by only considering p-p scatting (defined as  $\kappa_p^{p-p}$ ) and then further consider the effect of p-e coupling (the corresponding phononic thermal conductivity is defined as  $\kappa_{\rm p}^{\rm p-e}$ ). With BTE solutions, the mode level  $\kappa_{\rm p}^{\rm p-p}$  values for Pd, Ag, PbAuGa, and CsKNa are compared in Fig. 2(b). It is clearly seen that both the frequency range and frequency-dependent  $\kappa_{\rm p}^{\rm p-p}$  of PbAuGa and CsKNa are much lower than those for Pd and Ag, which is consistent with the

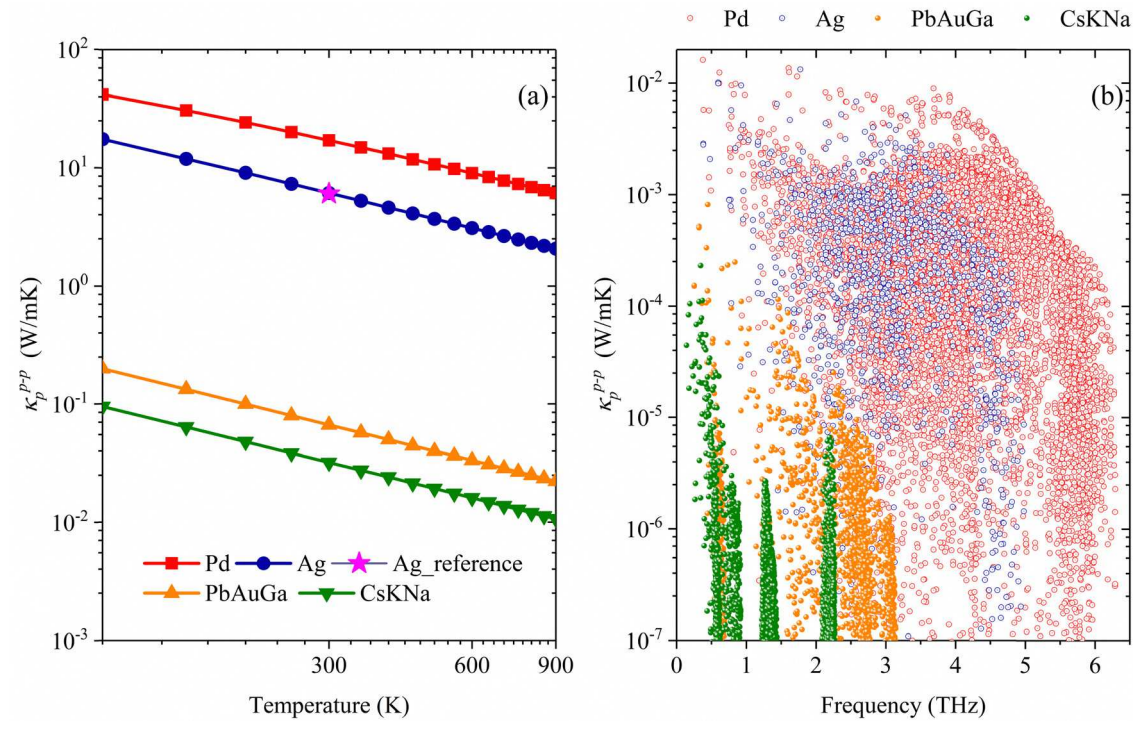


Fig. 2 Phononic thermal conductivity by only considering phonon-phonon scattering as a function of (a) temperature, and (b) frequency for Pd, Ag, PbAuGa, and CsKNa

 $\kappa_{\rm p}^{\rm p-p}$  variation trends of four systems. To observe how the  $\kappa_{\rm p}^{\rm p-p}$  changes with frequency, the cumulative  $\kappa_{\rm p}^{\rm p-p}$  values as a function of frequency for Pd, Ag, PbAuGa, and CsKNa are presented in Fig. S5 (ESI†). The cumulative  $\kappa_{\rm p}^{\rm p-p}$  values of all four systems increase with frequency, but the cumulative  $\kappa_p^{p-p}$  values of PbAuGa and CsKNa increase more steeply than those of Pd and Ag in the low frequency range. The acoustic modes of PbAuGa and CsKNa contribute the most to  $\kappa_{\rm p}^{\rm p-p}$ , being about 76% and 78%, respectively, and the contribution of LLO in PdAuGa and CsKNa to  $\kappa_p^{p-p}$  is about 19% and 10%, respectively. Fig. 2(b) also shows that compared with the other three systems where the frequency-dependent  $\kappa_{\rm p}^{\rm p-p}$  values are scattered in their respective entire frequency range, the frequencydependent  $\kappa_p^{p-p}$  values of CsKNa show pillar-like behavior. In particular, a large pillar occurs in the frequencies above 2 THz which is the HLO frequency range, which leads to considerable contribution of HLO in CsKNa (12%), higher than the counterpart of PdAuGa (5%).

Based on eqn (1), phononic thermal conductivity can be influenced by two important factors which quantify the effective movement of heat carriers: phonon velocity and phonon lifetime. From Fig. 3(a), we see the trend of group velocity:  $\bar{\nu}_{
m pd} > \bar{\nu}_{
m Ag} > \bar{\nu}_{
m PbAuGa} > \bar{\nu}_{
m CsKNa}$ , which is consistent with the trend of their phononic thermal conductivity shown in Fig. 2(a). As we all know, the phonon group velocity is given by the slope of the dispersion relation,  $^{35}$   $\nu = \partial \omega / \partial q$ . From the phonon dispersion shown in Fig. 1(c) and (d), it can be seen that the group velocity of PbAuGa is larger than that of CsKNa, which is

evidenced by the highly dispersive acoustic phonon branches in the vicinity of the  $\Gamma$ -point.

For further insight into the phonon lifetime induced by anharmonic interactions, the scattering phase space is computed, which is used to characterize the number of available phonon scattering channels. To explore and clarify the mechanism, the three-phonon scattering phase space  $(P_3)$  is calculated as:<sup>36</sup>

$$P_3 = \frac{2}{3\Omega} \left( P_3^{(+)} + \frac{1}{2} P_3^{(-)} \right) \tag{5}$$

$$P_3^{(\pm)} = \sum_{i} \int dq D_j^{(\pm)}(q)$$
 (6)

$$D_{j}^{(\pm)}(q) = \sum_{j',j''} \int \! \mathrm{d}q' \delta ig( \omega_{j}(q) \pm \omega_{j'}(q') - \omega_{j''}(q \pm q'' - G) ig) \quad (7)$$

where  $\Omega$  is the normalization factor. In eqn (6) and (7),  $D_i^{(\pm)}(q)$  is the two phonon density of states and momentum conservation which has already been imposed on q''.<sup>37</sup> According to eqn (5)–(7),  $P_3$  contains a large number of scattering events that satisfy the conservation conditions and can be used to quantitatively assess the number of scattering channels available for each phonon mode. Consequently, there is an inverse relationship between the intrinsic lattice thermal conductivity of a material and  $P_3$ .<sup>38</sup> The phase space of four systems is compared in Fig. 3(b). The phase space of PbAuGa and CsKNa is comparable to that of Pd and Ag, in particular for the phonon transport dominant acoustic frequency

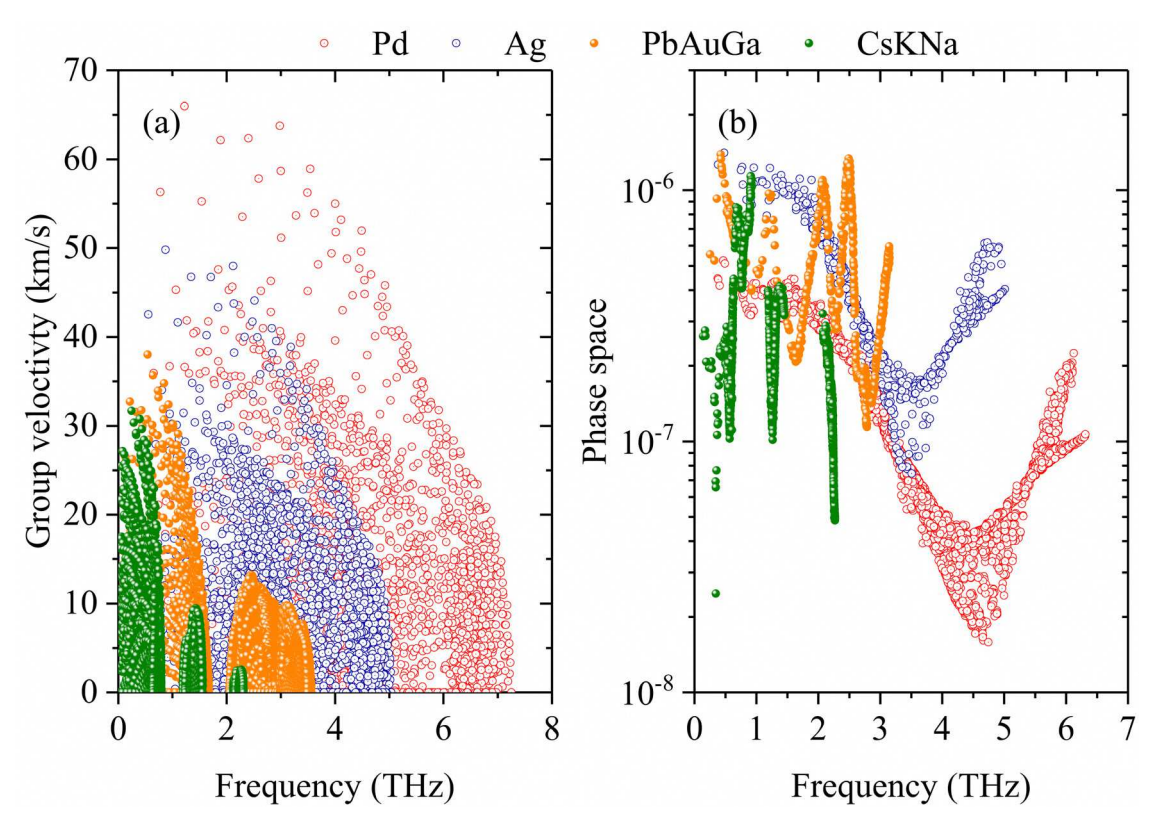


Fig. 3 Frequency-dependent group velocity (a) and phase space (b) of Pd, Ag, PbAuGa, and CsKNa

range. We can conclude that the number of scattering channels available for PbAuGa and CsKNa is not the major factor for their ultralow phononic thermal conductivity.

Now we turn to the phonon lifetime itself to reveal the underlying mechanism responsible for the ultralow  $\kappa_{\rm p}^{\rm p-p}$  of PbAuGa and CsKNa. As shown in Fig. 4, the lifetime of PbAuGa and CsKNa is at least one order of magnitude lower than that of Pd and Ag, in particular for the acoustic phonon modes, which agrees with the trend of phononic thermal conductivity. Interestingly, in the higher frequency range of the frequencydependent lifetime of CsKNa, there appears an unusual peak around 2 THz, which is associated with the phonon frequency gap-induced prohibition of phonon scattering channels [see Fig. 1(d)]. The contribution of the HLO mode to  $\kappa_p^{p-p}$  in CsKNa is high (12%), which can be ascribed to the second and broader phonon frequency gap between the LLO and HLO modes in CsKNa [see Fig. 1(d)]. Generally speaking, a broader frequency gap between different phonon modes restricts the scattering phase space by prohibiting possible three-phonon scatterings, since the energy criterion for phonon scattering ( $\omega_1 \pm \omega_2 = \omega_3$ ) would be hard to fulfill if there is a gap in dispersions. The phonon lifetime is inversely proportional to the number of scattering channels: the fewer the available scattering channels, the longer the phonon lifetime. 39,40 Comparing PbAuGa and CsKNa, the broader phonon frequency gap in the 1.5 to 2.1 THz range in CsKNa results in the higher contribution of HLO modes in CsKNa (12%) than that in PbAuGa (5%). In Fig. 4 we also show the Ioffe-Regel limit in lifetime,  $^{41}$  i.e.,  $\tau = 1/\omega$ , where  $\omega$  is the phonon frequency. Using the Ioffe-Regel criterion,42 this is the lowest limit for particle-like phonon transport, which means that the carrier scattering has reached the highest limit (correspondingly, the lifetime reaches the lowest limit). Compared with Pd and Ag, the lifetimes of PbAuGa and CsKNa almost approach the Ioffe-Regel limit, in particular for the acoustic phonon modes, indicating extremely

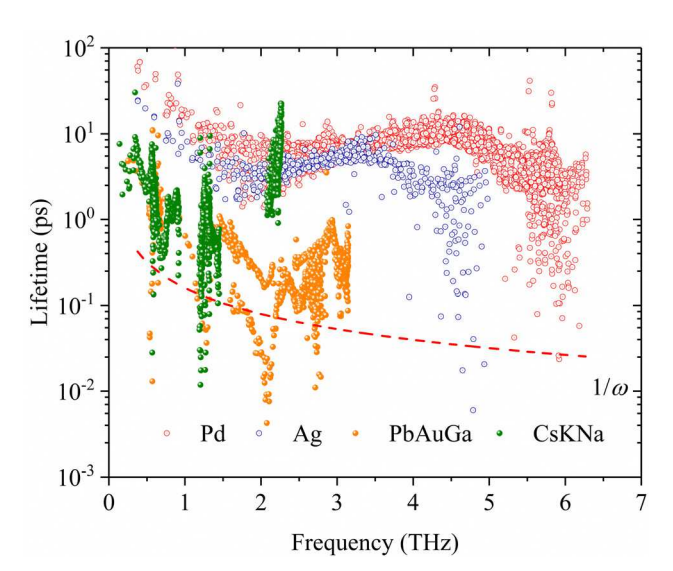


Fig. 4 Frequency-dependent phonon lifetime of Pd, Ag, PbAuGa, and CsKNa. The dashed line indicates the Ioffe-Regel limit (1/ $\omega$ ).

high phonon scattering and thus ultralow phononic thermal conductivity. Combining the above results, we conclude that the ultralow phononic thermal conductivity of PbAuGa and CsKNa is dominated by low group velocity and ultrashort lifetime.

It is well known that chemical bonding in crystal structures plays an important role in determining lattice thermal conductivity. 43-46 Since both PbAuGa and CsKNa are metallic [see the band structure in Fig. S2, ESI†], the metallic bonding will be the dominant interatomic interaction, and thus we will study the correlation between low phononic thermal conductivity and metallic bonding nature [see ELF in Fig. S7, ESI†]. As discussed earlier, the acoustic modes of PbAuGa and CsKNa contribute the most to  $\kappa_p^{p-p}$  (~76% and 75%, respectively), which originates from Au and Cs atoms, respectively. Therefore, we focus our analysis on the movement of Au and Cs atoms in PbAuGa and CsKNa, respectively, and its effect on the phonon scattering. To this end, we calculate mean square displacements (MSDs)<sup>47</sup> of representative atoms Pb, Ag, Au, and Cs in different systems with varying temperatures [see Fig. 5(a)]. This time the atoms do not stay in a fixed position but move randomly around the equilibrium positions. The MSD increases with the increase in temperature, but  $\kappa_p^{p-p}$  has an inverse relationship with MSD, i.e., the higher the MSD, the lower the  $\kappa_{\rm p}^{\rm p-p}$ , as also evidenced by our recent big data analysis on  $\sim$  29 000 cubic structures. <sup>22</sup> The MSDs of all atoms in CsKNa and PbAuGa are much higher than those of Pd and Ag atoms in pure metals. The higher MSD indicates that the atoms can do a periodic movement with large displacement away from their equilibrium position, and also implies that atoms are loosely bonded with neighbors and indeed act as intrinsic rattlers. It is known that the rattling effect is associated with increased phonon scattering, which is an important mechanism for reducing phononic thermal conductivity. 40 Comparing different elements in the same material, the MSDs of Au and Cs are higher than the rest of the atoms in PbAuGa and CsKNa, respectively. Therefore, the displacements of Au and Cs atoms are appreciable and comparable to previously reported guest rattler atoms, which induce strong phonon anharmonicity and finally the unusually low  $\kappa_p^{p-p}$  of PbAuGa and CsKNa. Moreover, the nature of the loose bonding in PbAuGa and CsKNa can be reflected by their low Young's modulus and shear modulus [see Table S3, ESI†]. Generally, materials with low Young's modulus and shear modulus would result in low phonon group velocity and thus low thermal conductivity.48

Furthermore, to study whether rattlers Au and Cs are loosely bonded with the neighbor atoms and move easily around the equilibrium positions, we calculated the potential energy change with respect to the displacement of atoms from their equilibrium positions. Among all three acoustic branches, the LA branch contributes the most to thermal conductivity, accounting for 52% of PbAuGa and 35% of CsKNa, respectively. Therefore, the eigenvector of the LA branch is chosen for the Au and Cs atomic vibration modes. The zero displacement factor on the x-axis means that the atom is at the equilibrium position, and the absolute value of the increasing displacement

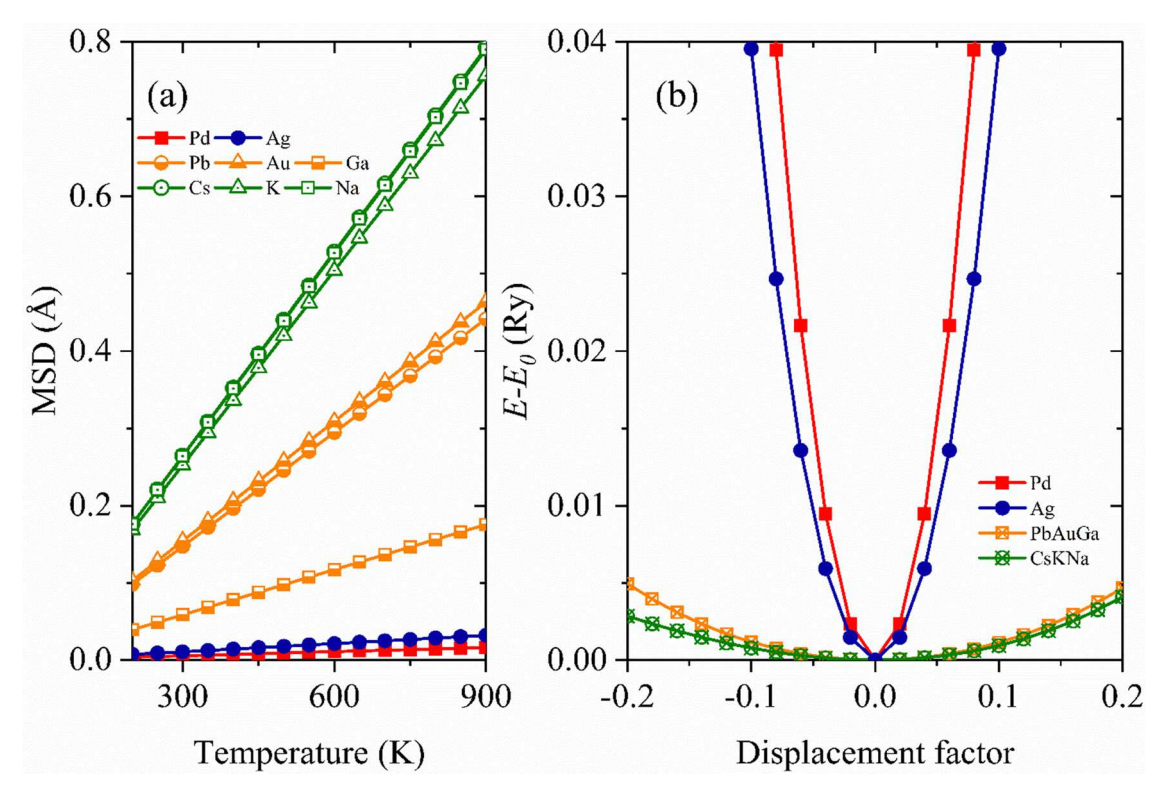


Fig. 5 (a) Comparison of mean square displacement (MSD) as a function of temperature among all elements in the four materials. (b) Comparison of potential energy as a function of the displacement factor.

factor means that the amplitude of the atom vibrates around the equilibrium position. While pure metals Pd and Ag lie in very deep potential wells, PbAuGa and CsKNa lie in very shallow potential wells, meaning that the Au and Cs atoms can fly far away from the equilibrium positions at the same temperature (thus with the same energy level of  $k_BT$ ). Furthermore, these shallow potential wells deviate from the perfect harmonic behavior [see Fig. S6, ESI†], indicating that Au and Cs atoms in PbAuGa and CsKNa, respectively, are indeed loosely bonded with neighbors and act as rattlers, which induce strong phonon anharmonicity and thus lower the  $\kappa_p^{p-p}$ .

It was recently found that MgCuSb possesses a non-centrosymmetric cubic structure (space group no. 216) which is the same as the structure types of PbAuGa and CsKNa. The intrinsic thermal conductivity of MgCuSb is also relatively low ( $\sim 3$  W mK<sup>-1</sup>). It was revealed that both the native strong anharmonicity induced by the tension effect of atomic filling and a low-energy shearing vibration mode triggered by weak Mg-Cu bonding are responsible for the unusually suppressed phonon conduction in MgCuSb. 49 In comparison, Au and Cs atoms in PbAuGa and CsKNa respectively act as the rattlers, and their physical binding feature accounts for the global weak bonding environment in PbAuGa and CsKNa [see Fig. S7, ESI†], which leads to a higher MSD than that of MgCuSb. In addition, the lifetimes of PbAuGa and CsKNa approach closer to the Ioffe-Regel limit which means stronger anharmonic atomic interaction in PbAuGa and CsKNa. Therefore, the lattice thermal conductivity of PbAuGa and CsKNa in our work is almost two orders of magnitude lower than MgCuSb.

To ascertain the bonding component, the Local-Orbital Basis Suite Towards Electric-Structure Reconstruction (LOBSTER)<sup>50,51</sup> package is used to obtain the crystal orbital Hamiltonian population (COHP) for interactions between selected atom pairs. In the valence band energy range (Fermi energy below 0 eV,  $\varepsilon_{\rm F}$  < 0 eV), bonding states are positive and anti-bonding states are negative.<sup>52</sup> The interactions in Au-Pb and Ga-Au have anti-bonding components, which are marked by the dashed rectangles in Fig. 6(b) and (c), indicating that the Au atom is loosely bonded to the lattice in the PbAuGa system. For the CsKNa system, the COHPs of K-Cs and Na-Cs are both negative, corresponding to the anti-bonding there [see dashed rectangles in Fig. 6(e) and (f)], therefore the Cs atom is loosely bonded to its surroundings as well. On account of Au and Cs that are evidently loosely bonded to the lattice, we naturally suspect that these atoms are highly prone to larger thermal fluctuations compared to other atoms in the lattice. Thus, by examining qualitative descriptors, the MSD, COHP, supplemented with the inference obtained from phonon dispersions, as well as quantitative descriptors in group velocity and lifetime, we verify that the loosely bound atoms Au and Cs act at the rattler atoms that suppress the  $\kappa_{\rm p}^{\rm p-p}$  of PbAuGa and CsKNa, respectively.

#### (2) Effect of phonon-electron coupling on phononic thermal conductivity

The p-e scattering is an important scattering mechanism in the phonon scattering process for metals and thus it should be rigorously considered in the two metallic materials herein. The  $\kappa_{\rm p}^{\rm p-p}$ ,  $\kappa_{\rm p}^{\rm p-e}$  (the phononic thermal conductivity after considering

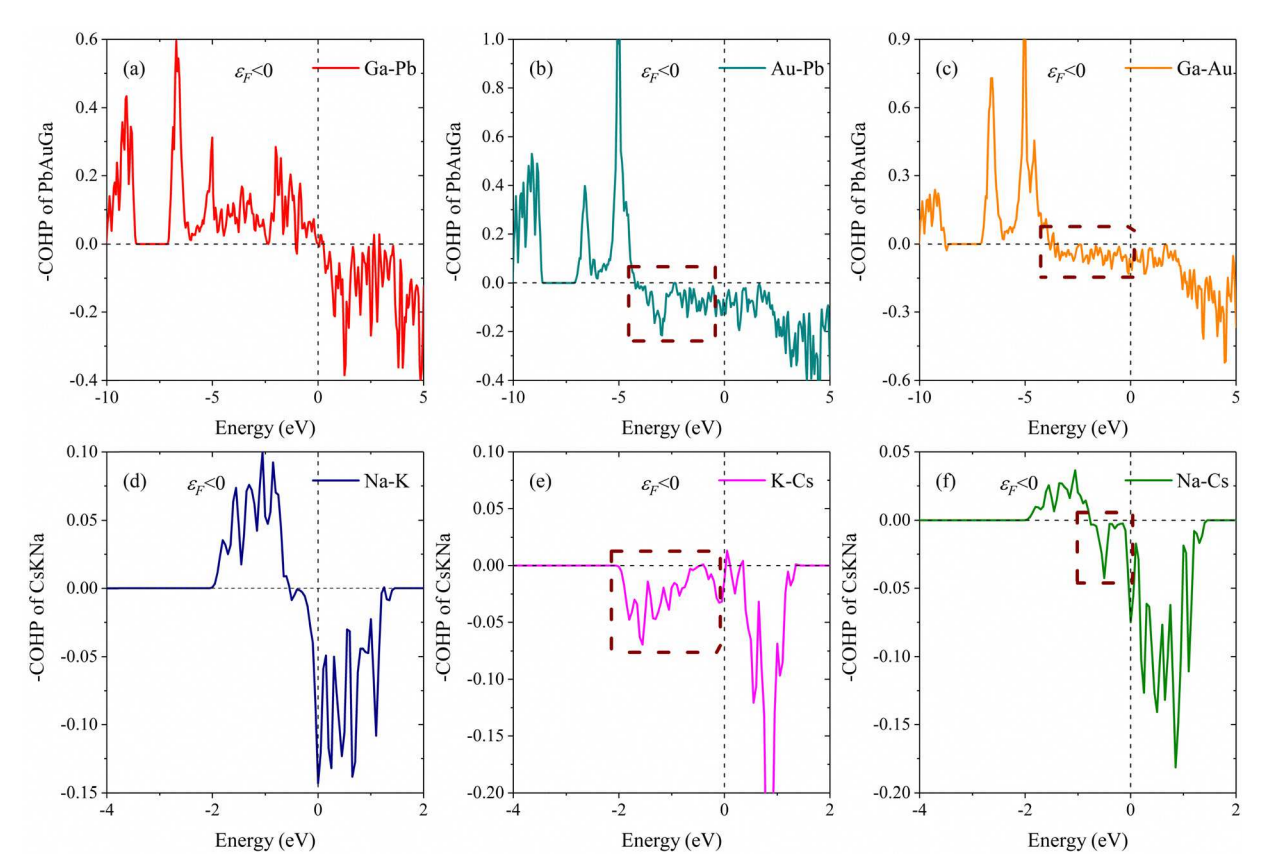


Fig. 6 Crystal orbital Hamiltonian populations (COHPs) for interactions between the selected atom pairs in PbAuGa (a)-(c) and CsKNa (d)-(f). The dashed rectangles indicate the anti-bonding components

phonon-electron coupling), and  $\kappa_e^{p-e}$  (the electronic thermal conductivity by considering phonon-electron coupling) of 21 pure metals and intermetallic compounds are compared in Table S5 (ESI†) (some raw data are taken from ref. 18). The total thermal conductivity  $(\kappa_{\text{total}}^{\text{DFT}} = \kappa_{\text{p}}^{\text{p-e}} + \kappa_{\text{e}}^{\text{p-e}})$  obtained by our DFT calculations for the pure metal Pd and Ag is 94.7 W mK<sup>-1</sup> and 402.35 W mK<sup>-1</sup>, respectively, which is in reasonable agreement with the experimental results (Pd: 71.7 W mK<sup>-1</sup>, Ag: 436 W mK<sup>-1</sup>).<sup>53</sup> Also, the  $\kappa_{\rm p}^{\rm p-e}$  of Ag is 5.86 W K<sup>-1</sup> by our calculation, which agrees well with the result (5.2 W mK<sup>-1</sup>) in the literature.<sup>54</sup> The above results evidently show that the process of our p-e coupling calculation is rigorous and reliable.

We first notice from Table S5 (ESI†) that the phononic thermal conductivity of PbAuGa and CsKNa does not change considerably before and after considering phonon-electron coupling, which is reflected by nearly no change in the phonon lifetime [see Fig. S8, ESI†] and this means that the electrons have the weakest effect on phonon transport in these two materials (3.03% and 3.13% for PbAuGa and CsKNa, respectively). This behavior is distinct from most of the pure metals and metallic structures shown in Fig. 7, where phonon-electron coupling has a significant effect on phonon transport in many systems. For instance, the  $(\kappa_p^{p-p} - \kappa_p^{p-e})/\kappa_p^{p-p}$  values of pure metals Pd and Ag are 29.28% and 4.09%, respectively, which are in good agreement with the previous literature. <sup>18</sup> The  $\kappa_{\rm p}^{\rm p-e}$  result also verifies that the root reason for the anomalously low

phononic thermal conductivity of PbAuGa and CsKNa is the loose bonding, inducing small group velocity and strong phonon anharmonicity. We also use  $\kappa_{\rm p}^{\rm p-e}/\kappa_{\rm total}^{\rm DFT}$  to quantify the percentage of the final phononic thermal conductivity contributing to total thermal conductivity. As shown by the orange bar in Fig. 7, generally speaking, the percentages of phononic thermal conductivity contributing to total thermal conductivity in metals and metallic materials are below 40%, which means that the electronic thermal conductivity possesses a higher contribution to overall thermal transport than the phononic counterpart. To be more specific, for pure metals Pd and Ag, phonons account for 15.05% and 1.46% of the total thermal conductivity, respectively, which is a reasonable range. However, the phononic thermal conductivity proportions of PbAuGa and CsKNa are only 0.37% and 0.29%, respectively, of the total thermal conductivity, meaning the phonon contribution in these two materials can be neglected and the thermal energy will be completely conducted by electrons. These percentages are several times lower than the other metallic materials shown in Fig. 7, and to the best of our knowledge, these phononic contribution percentages have reached the lowest level among all metals and metallic structures so far. It is worth noting that the  $\kappa_e^{p-e}$  of PbAuGa and CsKNa is 17.42 W mK<sup>-1</sup> and 10.76 W mK<sup>-1</sup>, respectively, which is in the lower region compared to many other pure metals and intermetallic materials between 7.34 W mK<sup>-1</sup> and 396.49 W mK<sup>-1</sup>. There are several effective methods that have been reported to suppress the

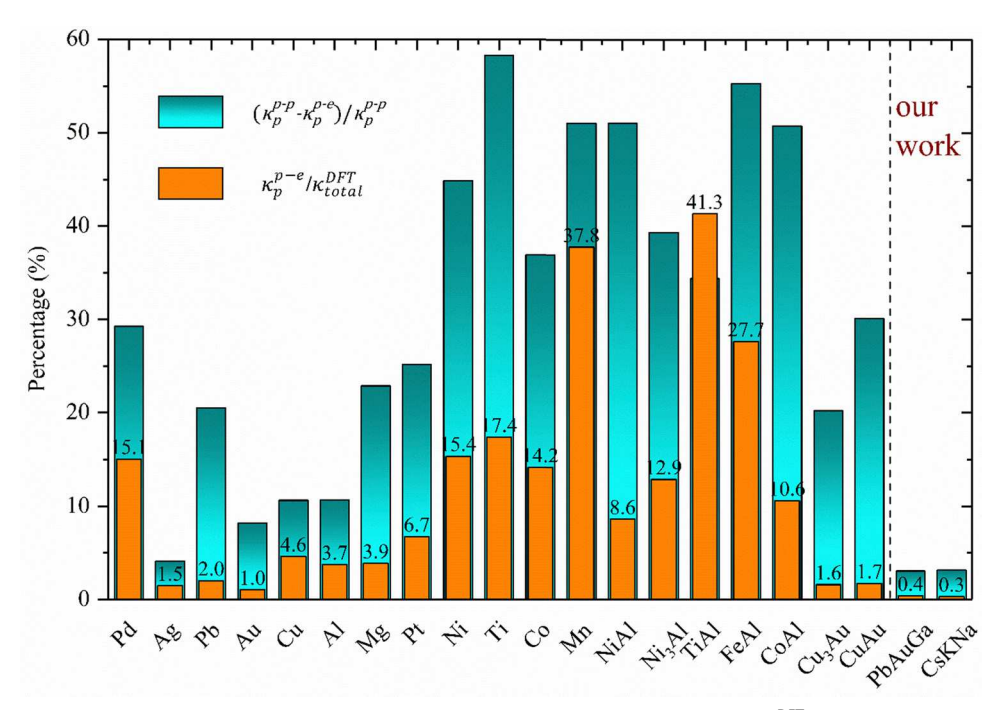


Fig. 7 Percentage of phononic thermal conductivity contribution to total thermal conductivity  $(\kappa_p^{\rm p-e}/\kappa_{\rm pt}^{\rm per})$  orange bar) and percentage of relative change in phononic thermal conductivity induced by the phonon–electron coupling effect  $((\kappa_p^{\rm p-p}-\kappa_p^{\rm p-e})/\kappa_p^{\rm p-p})$ , dark cyan bar). The numbers indicate the percentage of phononic thermal conductivity contribution to overall thermal transport.

electronic contribution to thermal conductivity, <sup>55,56</sup> *e.g.*, by substituting Te with Se in Ge<sub>2</sub>Sb<sub>2</sub>Te<sub>5</sub> composition, a drastic reduction in the electronic lifetime is experimentally observed in Ge<sub>2</sub>Sb<sub>2</sub>-Se<sub>4</sub>Te. <sup>56</sup> We speculate that PbAuGa and CsKNa may be applied as thermal insulators, by substituting the non-rattling atoms. It is also worth mentioning that the trend of electronic thermal conductivity corresponds with electrical conductivity, which is associated with the carrier concentration.

#### 4. Conclusions

In summary, first-principles calculations combined with phonon BTE are performed to systematically investigate the thermal transport in two cubic metallic materials, namely PbAuGa and CsKNa, by considering both phonon-phonon and phononelectron interactions. At room temperature, the phononic thermal conductivities of PbAuGa and CsKNa are only 0.064 W mK<sup>-1</sup> and 0.031 W mK<sup>-1</sup>, respectively, which are on the same order of magnitude as air (0.025 W mK<sup>-1</sup>). The phonons only contribute 0.37% and 0.29% to the total thermal transport, which is far below the normal range of other metals and metallic systems (1% to 40%). The analysis of phonon mode level properties reveals that the acoustic modes of PbAuGa and CsKNa originating from Au and Cs respectively contribute the most (about 76% and 78%) to  $\kappa_p^{p-p}$ . The trend of group velocity Pd, Ag, PbAuGa, and CsKNa is consistent with the trend of thermal conductivity, and the lifetimes of PbAuGa and CsKNa almost reach the Ioffe-Regel limit. Therefore, we conclude that the ultralow phononic thermal conductivity of PbAuGa and CsKNa is determined by low group velocity and strong anharmonic interaction. Furthermore, by qualitatively examining MSD, potential energy well, and COHP, we verify that the Au and Cs atoms act as the rattlers in PbAuGa and CsKNa, respectively, due to their loose bonding with neighbors, and thus suppress the phononic thermal conductivity of PbAuGa and CsKNa to the lowest level ever. Finally, the effect of phonon–electron coupling on the phononic thermal conductivity of PbAuGa and CsKNa is found to be very limited. This study deepens our understanding of heat conduction in metals and metallic systems and offers a new route for future emergent applications wherever blocking phonon transport to a large extent is desired.

## Data availability

The main data supporting the findings of this study are available within the paper and its ESI.† Other data are available from the corresponding authors upon request.

# Code availability

All codes used are available from the corresponding authors upon request.

#### Author contributions

M. H. conveyed the idea and designed and supervised the study. Z. Y., W. N., and A. R. performed the DFT calculations. L. L., J. W., K.Y. and Y. Y. analyzed the results. Z. Y. prepared the draft of the manuscript. K. Y., Y. Y., and M. H. revised the

manuscript. All the authors contributed to discussions and interpretation of results in the manuscript.

#### Conflicts of interest

The authors declare no competing interests.

#### Acknowledgements

This project is supported by the program of Educational Department of Liaoning Province (grant no. LQGD2020008, 20180540122, and SYJG20222014). J. W. acknowledges the support from the Key Program of Educational Department of Liaoning Province (no. LZGD2020004). K. Y. acknowledges the support from the National Natural Science Foundation of China (no. 52206219) and the China Postdoctoral Science Foundation (no. 2022M720636). Research reported in this publication was supported in part by the NSF (award number 2030128, 2110033, and 2320292), the SC EPSCoR Program under award number (23-GC01), and an ASPIRE grant from the Office of the Vice President for Research at the University of South Carolina (project 80005046). The DFT calculation was carried out at the Shanxi Supercomputing Center of China and TianHe-2.

#### References

- 1 L. Shi, C. Dames, J. R. Lukes, P. Reddy, J. Duda, D. G. Cahill, J. Lee, A. Marconnet, K. E. Goodson, J.-H. Bahk, A. Shakouri, R. S. Prasher, J. Felts, W. P. King, B. Han and J. C. Bischof, Evaluating Broader Impacts of Nanoscale Thermal Transport Research, Nanoscale Microscale Thermophys. Eng., 2015, 19(2), 127-165.
- 2 C. Chang and L.-D. Zhao, Anharmoncity and low thermal conductivity in thermoelectrics, Mater. Today Phys., 2018, 4,
- 3 J. W. L. Pang, W. J. L. Buyers, A. Chernatynskiy, M. D. Lumsden, B. C. Larson and S. R. Phillpot, Phonon Lifetime Investigation of Anharmonicity and Thermal Conductivity of UO2 by Neutron Scattering and Theory, Phys. Rev. Lett., 2013, 110(15), 157401.
- 4 L. D. Whalley, J. M. Skelton, J. M. Frost and A. Walsh, Phonon anharmonicity, lifetimes, and thermal transport in CH<sub>3</sub>NH<sub>3</sub>PbI<sub>3</sub> from many-body perturbation theory, *Phys.* Rev. B, 2016, 94(22), 220301.
- 5 J. Li, W. Zhai, C. Zhang, Y. Yan, P.-F. Liu and G. Yang, Anharmonicity and ultralow thermal conductivity in layered oxychalcogenides BiAgOCh (Ch = S, Se, and Te), Mater. Adv., 2021, 2(14), 4876-4882.
- 6 B. C. Sales, D. Mandrus and R. K. Williams, Filled Skutterudite Antimonides: A New Class of Thermoelectric Materials, Science, 1996, 272(5266), 1325-1328.
- 7 G. S. Nolas, T. J. R. Weakley, J. L. Cohn and R. Sharma, Structural properties and thermal conductivity of crystalline

- Ge clathrates, Phys. Rev. B: Condens. Matter Mater. Phys., 2000, 61(6), 3845-3850.
- 8 Z. Liu, W. Zhang, W. Gao and T. Mori, A material catalogue with glass-like thermal conductivity mediated by crystallographic occupancy for thermoelectric application, Energy Environ. Sci., 2021, 14(6), 3579-3587.
- 9 R. Juneja and A. K. Singh, Rattling-Induced Ultralow Thermal Conductivity Leading to Exceptional Thermoelectric Performance in AgIn<sub>5</sub>S<sub>8</sub>, ACS Appl. Mater. Interfaces, 2019, **11**(37), 33894-33900.
- 10 J. Li, W. Hu and J. Yang, High-Throughput Screening of Rattling-Induced Ultralow Lattice Thermal Conductivity in Semiconductors, J. Am. Chem. Soc., 2022, 144(10), 4448-4456.
- 11 J. Qi, B. Dong, Z. Zhang, Z. Zhang, Y. Chen, Q. Zhang, S. Danilkin, X. Chen, J. He, L. Fu, X. Jiang, G. Chai, S. Hiroi, K. Ohara, Z. Zhang, W. Ren, T. Yang, J. Zhou, S. Osami, J. He, D. Yu, B. Li and Z. Zhang, Dimer rattling mode induced low thermal conductivity in an excellent acoustic conductor, Nat. Commun., 2020, 11(1), 5197.
- 12 S. Chung, M. Tomita, R. Yokogawa, A. Ogura and T. Watanabe, Atomic mass dependency of a localized phonon mode in SiGe alloys, AIP Adv., 2021, 11, 115225.
- 13 Y. Lee, A. J. Pak and G. S. Hwang, What is the thermal conductivity limit of silicon germanium alloys?, Phys. Chem. Chem. Phys., 2016, 18(29), 19544-19548.
- 14 C. Shen, N. Hadaeghi, H. Singh, T. Long, L. Fan, G. Qin and H. Zhang, Anomalously low thermal conductivity of two-dimensional GaP monolayers: A comparative study of the group GaX (X = N, P, As), arXiv, arXiv:2107.09964 [cond-mat.mtrl-sci], 2021.
- 15 E. S. Toberer, C. A. Cox, S. R. Brown, T. Ikeda, A. F. May, S. M. Kauzlarich and G. J. Snyder, Traversing the Metal-Insulator Transition in a Zintl Phase: Rational Enhancement of Thermoelectric Efficiency in  $Yb_{14}Mn_{1-x}Al_xSb_{11}$ , Adv. Funct. Mater., 2008, 18, 2795-2800.
- 16 E. S. Toberer, A. Zevalkink and G. J. Snyder, Phonon engineering through crystal chemistry, J. Mater. Chem., 2011, 21, 15843-15852.
- 17 P. G. Klemens and R. K. Williams, Thermal conductivity of metals and alloys, Int. Met. Rev., 1986, 31(1), 197-215.
- 18 Z. Tong, S. Li, X. Ruan and H. Bao, Comprehensive firstprinciples analysis of phonon thermal conductivity and electron-phonon coupling in different metals, Phys. Rev. B, 2019, **100**(14), 144306.
- 19 T. A. R. Purcell, M. Scheffler, L. M. Ghiringhelli and C. Carbogno, Accelerating materials-space exploration for thermal insulators by mapping materials properties via artificial intelligence, npj Comput. Mater., 2023, 9(1), 112.
- 20 J. Ojih, U. Onyekpe, A. Rodriguez, J. Hu, C. Peng and M. Hu, Machine Learning Accelerated Discovery of Promising Thermal Energy Storage Materials with High Heat Capacity, ACS Appl. Mater. Interfaces, 2022, 14(38), 43277-43289.
- 21 G. Qin, Y. Wei, L. Yu, J. Xu, J. Ojih, A. D. Rodriguez, H. Wang, Z. Qin and M. Hu, Predicting lattice thermal conductivity from fundamental material properties using machine learning techniques, J. Mater. Chem. A, 2023, 11(11), 5801-5810.

- 22 A. Rodriguez, C. Lin, H. Yang, M. Al-Fahdi, C. Shen, K. Choudhary, Y. Zhao, J. Hu, B. Cao, H. Zhang and M. Hu, Million-scale data integrated deep neural network for phonon properties of heuslers spanning the periodic table, *npj Comput. Mater.*, 2023, 9(1), 20.
- 23 A. Rodriguez, C. Lin, C. Shen, K. Yuan, M. Al-Fahdi, X. Zhang, H. Zhang and M. Hu, Unlocking phonon properties of a large and diverse set of cubic crystals by indirect bottom-up machine learning approach, *Commun. Mater.*, 2023, 4(1), 61.
- 24 A. Jain, S. P. Ong, G. Hautier, W. Chen, W. D. Richards, S. Dacek, S. Cholia, D. Gunter, D. Skinner, G. Ceder and K. A. Persson, Commentary: The Materials Project: A materials genome approach to accelerating materials innovation, *APL Mater.*, 2013, 1(1), 011002.
- 25 S. Kirklin, J. E. Saal, B. Meredig, A. Thompson, J. W. Doak, M. Aykol, S. Rühl and C. Wolverton, The Open Quantum Materials Database (OQMD): assessing the accuracy of DFT formation energies, npj Comput. Mater., 2015, 1(1), 15010.
- 26 P. Giannozzi, S. Baroni, N. Bonini, M. Calandra, R. Car, C. Cavazzoni, D. Ceresoli, G. L. Chiarotti, M. Cococcioni, I. Dabo, A. Dal Corso, S. De Gironcoli, S. Fabris, G. Fratesi, R. Gebauer, U. Gerstmann, C. Gougoussis, A. Kokalj, M. Lazzeri, L. Martin-Samos, N. Marzari, F. Mauri, R. Mazzarello, S. Paolini, A. Pasquarello, L. Paulatto, C. Sbraccia, S. Scandolo, G. Sclauzero, A. P. Seitsonen, A. Smogunov, P. Umari and R. M. Wentzcovitch, QUANTUM ESPRESSO: a modular and open-source software project for quantum simulations of materials, J. Phys.: Condens. Matter, 2009, 21(39), 395502.
- 27 F. Zhou, W. Nielson, Y. Xia and V. Ozolinš, Lattice Anharmonicity and Thermal Conductivity from Compressive Sensing of First-Principles Calculations, *Phys. Rev. Lett.*, 2014, 113(18), 185501.
- 28 S. Lee, K. Esfarjani, T. Luo, J. Zhou, Z. Tian and G. Chen, Resonant bonding leads to low lattice thermal conductivity, *Nat. Commun.*, 2014, 5(1), 3525.
- 29 S. Poncé, E. R. Margine, C. Verdi and F. Giustino, EPW: Electron-phonon coupling, transport and superconducting properties using maximally localized Wannier functions, *Comput. Phys. Commun.*, 2016, 209, 116–133.
- 30 W. Li, J. Carrete, N. Katcho and N. Mingo, ShengBTE: A solver of the Boltzmann transport equation for phonons, *Comput. Phys. Commun.*, 2014, **185**, 1747–1758.
- 31 A. Giri, A. Z. Chen, A. Mattoni, K. Aryana, D. Zhang, X. Hu, S.-H. Lee, J. J. Choi and P. E. Hopkins, Ultralow Thermal Conductivity of Two-Dimensional Metal Halide Perovskites, *Nano Lett.*, 2020, **20**(5), 3331–3337.
- 32 J. Sun, M. Hu, C. Zhang, L. Bai, C. Zhang and Q. Wang, Ultralow Thermal Conductivity of Layered Bi<sub>2</sub>O<sub>2</sub>Se Induced by Twisting, *Adv. Funct. Mater.*, 2022, 32(47), 2209000.
- 33 Y. Zhou, S. Xiong, X. Zhang, S. Volz and M. Hu, Thermal transport crossover from crystalline to partial-crystalline partial-liquid state, *Nat. Commun.*, 2018, **9**(1), 4712.
- 34 M. Al-Fahdi, X. Zhang and M. Hu, Phonon transport anomaly in metavalent bonded materials: contradictory to the conventional theory, *J. Mater. Sci.*, 2021, 56.

- 35 X. Cong, Q.-Q. Li, X. Zhang, M.-L. Lin, J.-B. Wu, X.-L. Liu, P. Venezuela and P.-H. Tan, Probing the acoustic phonon dispersion and sound velocity of graphene by Raman spectroscopy, *Carbon*, 2019, **149**, 19–24.
- 36 L. Lindsay and D. A. Broido, Three-phonon phase space and lattice thermal conductivity in semiconductors, *J. Phys.: Condens. Matter*, 2008, **20**(16), 165209.
- 37 K. Okubo and S.-I. Tamura, Two-phonon density of states and anharmonic decay of large-wave-vector LA phonons, *Phys. Rev. B: Condens. Matter Mater. Phys.*, 1983, **28**(8), 4847–4850.
- 38 B. Peng, H. Zhang, H. Shao, Y. Xu, X. Zhang and H. Zhu, Low lattice thermal conductivity of stanene, *Sci. Rep.*, 2016, 6(1), 20225.
- 39 K. Yuan, X. Zhang, Z. Chang, Z. Yang and D. Tang, Pressure-Induced Anisotropic to Isotropic Thermal Transport and Promising Thermoelectric Performance in Layered InSe, ACS Appl. Energy Mater., 2022, 5(9), 10690–10701.
- 40 U. Singh, S. Singh, M. Zeeshan, J. van den Brink and H. C. Kandpal, Low lattice thermal conductivity in alkali metal based Heusler alloys, *Phys. Rev. Mater.*, 2022, 6(12), 125401.
- 41 P. Sheng, M. Zhou and Z.-Q. Zhang, Phonon transport in strong-scattering media, *Phys. Rev. Lett.*, 1994, 72(2), 234–237.
- 42 M. Gurvitch, Ioffe-Regel criterion and resistivity of metals, *Phys. Rev. B: Condens. Matter Mater. Phys.*, 1981, **24**(12), 7404-7407.
- 43 L. Elalfy, D. Music and M. Hu, Metavalent bonding induced abnormal phonon transport in diamondlike structures: Beyond conventional theory, *Phys. Rev. B*, 2021, **103**(7), 075203.
- 44 G. Qin, Z. Qin, H. Wang and M. Hu, Lone-pair electrons induced anomalous enhancement of thermal transport in strained planar two-dimensional materials, *Nano Energy*, 2018, **50**, 425–430.
- 45 H. Wang, G. Qin, J. Yang, Z. Qin, Y. Yao, Q. Wang and M. Hu, First-principles study of electronic, optical and thermal transport properties of group III–VI monolayer MX (M = Ga, In; X = S, Se), *J. Appl. Phys.*, 2019, 125(24), 245104.
- 46 K. Yuan, X. Zhang, D. Tang and M. Hu, Anomalous pressure effect on the thermal conductivity of ZnO, GaN, and AlN from first-principles calculations, *Phys. Rev. B*, 2018, **98**(14), 144303.
- 47 L. Zhou, J. Zhu, Y. Zhao and H. Ma, A molecular dynamics study on thermal conductivity enhancement mechanism of nanofluids – Effect of nanoparticle aggregation, *Int. J. Heat Mass Transfer*, 2022, 183, 122124.
- 48 Y. Shen, F. Q. Wang and Q. Wang, Ultralow thermal conductivity and negative thermal expansion of CuSCN, *Nano Energy*, 2020, 73, 104822.
- 49 J. Zhu, L. Xie, Z. Ti, J. Li, M. Guo, X. Zhang, P.-F. Liu, L. Tao, Z. Liu, Y. Zhang and J. Sui, Computational understanding and prediction of 8-electron half-Heusler compounds with unusual suppressed phonon conduction, *Appl. Phys. Rev.*, 2023, 10(3), 031405.
- 50 R. Dronskowski and P. E. Bloechl, Crystal orbital Hamilton populations (COHP): energy-resolved visualization of

- chemical bonding in solids based on density-functional calculations, J. Phys. Chem., 1993, 97(33), 8617-8624.
- 51 V. L. Deringer, A. L. Tchougréeff and R. Dronskowski, Crystal Orbital Hamilton Population (COHP) Analysis As Projected from Plane-Wave Basis Sets, J. Phys. Chem. A, 2011, 115(21), 5461-5466.
- 52 J. Ding, T. Lanigan-Atkins, M. Calderón-Cueva, A. Banerjee, D. L. Abernathy, A. Said, A. Zevalkink and O. Delaire, Soft anharmonic phonons and ultralow thermal conductivity in Mg<sub>3</sub>(Sb, Bi)<sub>2</sub> thermoelectrics, Sci. Adv., 2021, 7(21), eabg1449.
- 53 R. W. Powell and Y. S. Touloukian, Thermal Conductivities of the Elements, Science, 1973, 181(4104), 999-1008.

- 54 Y. Wang, Z. Lu and X. Ruan, First principles calculation of lattice thermal conductivity of metals considering phononphonon and phonon-electron scattering, J. Appl. Phys., 2016, 119(22), 225109.
- 55 C. V. Manzano, O. Caballero-calero, M. Tranchant, E. Bertero, P. Cervino-Solana, M. Martin-Gonzalez and L. Philippe, Thermal conductivity reduction by nanostructuration in electrodeposited CuNi alloys, J. Mater. Chem. C, 2021, 9(10), 3447-3454.
- 56 K. Aryana, Y. Zhang, J. A. Tomko, M. S. B. Hoque, E. R. Hoglund, D. H. Olson, J. Nag, J. C. Read, C. Ríos, J. Hu and P. E. Hopkins, Suppressed electronic contribution in thermal conductivity of Ge<sub>2</sub>Sb<sub>2</sub>Se<sub>4</sub>Te, Nat. Commun., 2021, 12(1), 7187.